

Dynamic features of ion guiding by nanocapillaries in an insulating polymer

Y. Kanai,^{1,*} M. Hoshino,² T. Kambara,³ T. Ikeda,¹ R. Hellhammer,⁴ N. Stolterfoht,⁴ and Y. Yamazaki^{1,5}

¹Atomic Physics Lab., RIKEN, Wako, Saitama 351-0198, Japan

²Department of Physics, Sophia University, Chiyoda, Tokyo 102-8554, Japan

³Nishina Center, RIKEN, Wako, Saitama 351-0198, Japan

⁴Helmholtz-Zentrum Berlin für Materialien und Energie, Glienickstrasse 100, D-14109 Berlin, Germany

⁵Institute of Physics, University of Tokyo, Komaba, Meguro, Tokyo 153-8902, Japan

(Received 22 October 2008; published 23 January 2009)

Dynamic features of the guiding of Ne^{7+} ions through nanocapillaries in insulating PET polymers were investigated for incident energies from 3.5 to 7 keV. The deflection angle of the transmitted Ne^{7+} ions shows a few oscillations before approaching an equilibrium value. The experimental results are interpreted in terms of a scenario where the deflection angles of transmitted ions are governed by charge patches formed on the inner wall of the capillary. In addition, the memory effects of different charge patches retained from previous irradiations are studied.

DOI: 10.1103/PhysRevA.79.012711

PACS number(s): 34.50.Fa, 32.80.Fb

I. INTRODUCTION

Interactions between slow highly charged ions (HCIs) and solid surfaces have extensively been studied experimentally and theoretically [1–3]. HCI-metal surface interactions, especially charge transfer processes from the metallic surface, can be well explained by the so-called classical over-the-barrier model [4]. With metallic microcapillary target, experimental evidence of hollow ions in vacuum and the related charge transfer processes have been shown [5,6]. On the other hand, interactions between ions and insulator surfaces have complex features, which depend on the insulator surface properties.

Recently, Stolterfoht *et al.* [7] showed that mesoscopic properties of the insulator surface can be used to guide slow ions along the capillary axis of an insulator nanocapillary. Qualitatively, this phenomenon can be explained as follows [7,8]: (1) ions collide with inner wall of a nanocapillary and a positive charge patch is formed near the entrance region, (2) following ions are deflected by the charge patch into the capillary axis direction, and (3) a considerable number of ions are transmitted through the nanocapillary without any close collisions with the inner wall.

Until now, various kinds of insulator capillaries (multi-capillaries [7,9–11] and single-glass capillaries [12,13]) have been used to demonstrate the ion guiding effect. Especially for nanocapillaries in a PET foil, ion guiding properties in equilibrium conditions, i.e., after the saturation of the transmitted ion intensity, were reported and the relationship between the guiding power and the width of the transmission profile was revealed [14,15]. In such experiments, using a one-dimensional detector, it is rather difficult to measure the two-dimensional angular profiles of transmitted ions changing with time.

In this work, we utilize a two-dimensional (2D) position sensitive detector (PSD) to measure the transmitted ions. Position and time information of the ions hitting the 2D PSD

was recorded by a list mode. This method [16–19] allows us to measure the spatial change of the transmitted ions in step of a few seconds, which is the minimum time for accumulation of enough signals to produce a clear 2D image. We have observed the spatial change (peak shape and deflected direction) of the transmitted ions, which provides information about the time evolution of the charging up of the capillary inner wall. We refer to it as the dynamic features of ion guiding phenomena. Our experimental results are consistent with theoretical simulations [8,20].

II. EXPERIMENTS

We performed the experiments at RIKEN with Ne^{7+} ions from a 14.5 GHz electron cyclotron resonance (ECR) ion source [21]. The beam energies were between 3.5 and 7 keV, and the beam intensity ranged from 5 to 200 pA at the target position. The beam divergence was smaller than 0.5° , and the size of the beam at the target was 1–1.5 mm in diameter. The vacuum in the chamber was better than 1×10^{-5} Pa. The experimental setup is shown in Fig. 1. A polyethylene terephthalate (PET) foil was attached to the target holder, which can be rotated by the angles ψ and χ as shown in Fig. 1. Angles of ψ and χ were measured from the beam direction. The PET foil included capillaries with a length of 12 μm and a diameter of 200 nm. The capillary density was

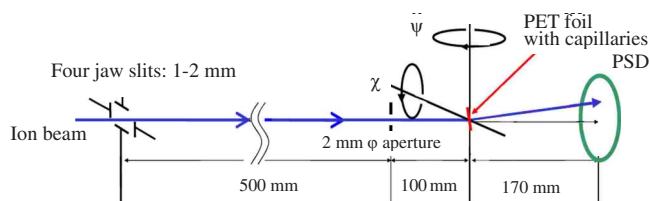


FIG. 1. (Color online) Experimental setup. Ne^{7+} ions are collimated by four jaw slits and a 2 mm aperture before the target, which can be rotated by the angles ψ and χ as indicated. Transmitted ions are measured by a 2D position sensitive detector (PSD). An electrostatic deflector can be set just after the target to analyze the charge state of the transmitted ions.

*kanaiyasuyuki@riken.jp

4×10^6 holes/cm², which was two orders of magnitude lower than that of the target used in previous experiments [7,9]. To avoid charging up of the PET foil surface, Au was evaporated under 30° on the front and back sides of the PET foil. The Au layer reaches about 150 nm into the entrance and exit regions of the capillaries [7]. It is noted that when an electron shower was used to avoid a macroscopic charging up of an Al₂O₃ multicapillary target, it behaved just like a metallic capillary target, and no guiding effect was observed because the electron shower prevented not only the macroscopic charging up of the target surface but also the microscopic charging up of inner wall of each capillary tunnel [22].

A two-dimensional (2D) position sensitive detector (PSD), which consists of micro-channel plates and a wedge and strip anode is located 170 mm away from the target position. An electrostatic deflector can be set just after the target position, to analyze the charge state of the transmitted ions. The electric field of the deflector is parallel with the ψ direction. We have measured the transmitted ions by the 2D PSD as a function of time with a constant ion current. The information about the ion hitting the 2D PSD including its position and the time, and also the ion current at the PET foil were recorded by a PC using a list mode. This allows us to measure the change of the profile and position of transmitted ions as a function of charge Q_d deposited on the PET surface. The deposited charge Q_d is a proper parameter to discuss the intensity evolution of the guided ions [17].

In the present study, we studied the dynamic behavior of the guiding effect for two different initial conditions. (a) “Fresh” surface: to study the charging up processes on the inner wall, we performed experiments with a fresh surface condition. In this case the capillary inner wall was expected to hold no charge. To realize such condition, we waited about one week after the previous experiment. According to recent studies [7,18] and our own preliminary measurements, the characteristic discharge time of the charge patch in the capillary is of the order of 1–3 h. One week is expected to be enough to erase the previous memory on charge at the inner wall of the PET capillary. (b) “Charged” surface: to study the charging up processes in conjunction with the remaining charge patches produced by precharging before the experiment.

III. RESULTS AND DISCUSSION

Figure 2 shows a typical example of the intensity evolution of the transmitted ions as a function of Q_d . Moreover, a couple of 2D images of the ions are depicted to demonstrate the profile and position of the transmitted ions during the intensity evolution. Here, the charge states of the transmitted ions are analyzed. Expected positions of Ne and Ne⁷⁺ are shown by the arrows in Fig. 2. When the irradiation starts, only a weak neutral Ne peak is observed. As Q_d increases, the Ne⁷⁺ peak quickly increases. In the equilibrium condition, i.e., after the intensity saturation, a small number of ions with charge states between 0 and 6 are also observed although more than 90% of the transmitted ions are Ne⁷⁺.

Neutral neon and charge states smaller than 7 may be produced in glancing collisions of Ne⁷⁺ ions with the inner

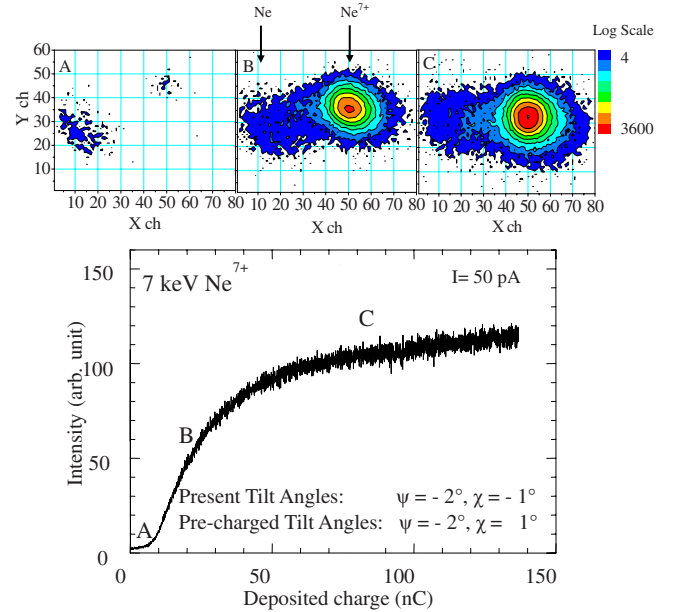


FIG. 2. (Color online) Typical evolution of the integrated intensity and the 2D images of the transmitted ions as a function of charge Q_d deposited on the PET surface. 2D images for different deposited charge Q_d are shown: A for $Q_d=0-5$ nC, B for $Q_d=20-25$ nC, and C for $Q_d=80-85$ nC. Here, an electrostatic deflector was set just after the target. Expected positions for different charge states of the ions are shown by arrows. In these 2D images the number of 11ch corresponds to 1° .

wall and/or the exit of the capillaries. One possible mechanism is multiple charge transfer processes from the Au layer near the exit of capillaries, which is similar to that for the ion-metallic capillary interactions [23].

During the evolution of the intensity, the 2D images of transmitted ions vary as seen in Fig. 2. Note that the labels A, B, and C for the upper graphs correspond to those given in the lower graph. As is seen in Fig. 2, the average deflection angle varies with Q_d . These changes show that the charge patches of the capillary inner wall evolve. In Fig. 2, the peak position moves along the Y axis, which corresponds to the χ direction. The direction of this shift is determined by a “memory effect” of the precharged capillary inner wall, which will be discussed later.

During the intensity evolution, the shape of the transmitted ion profile also changes. In the equilibrium, the shape of the transmitted ion profile is almost circular and the angular width is about 1° [16]. The angular widths of the transmitted ions depend on the beam energy [16] as reported previously [9,15]: the higher the beam energy, the smaller the angular width.

We have to mention that the absolute angular width $\sim 1^\circ$ of the transmitted ions of the present experiments [16] with the capillary density of 4×10^6 holes/cm² is much smaller than the value of 5° reported in previous measurements [7] with the higher capillary density of some 10^8 holes/cm². This difference may partially be explained by the difference of the capillary density.

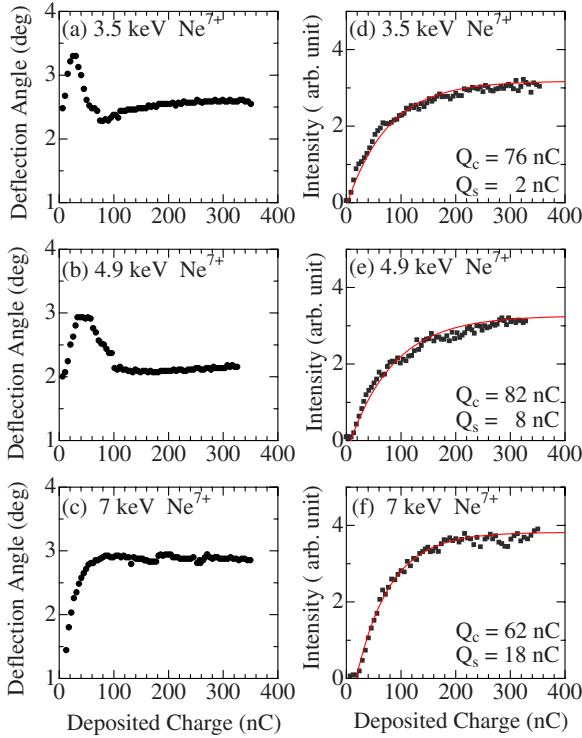


FIG. 3. (Color online) Deflection angles (χ direction) and intensity evolutions of Ne^{7+} ions transmitted through a fresh sample. The tilt angles were $\psi=0^\circ$ and $\chi=2.8^\circ$. The ion energies are 3.5 (a), (d); 4.9 (b), (e); and 7 (c), (f) keV. The ion current is 50 pA. The data are given as functions of charge Q_d deposited on the PET surface. The intensity evolution for each energy was fitted by the function of $I(Q_d)=I_{max}\{1-\exp[-(Q_d-Q_s)/Q_c]\}$ [14,15]. The fitted function (red curves) and the values of Q_c and Q_s are shown in figures. The 0° determination of the deflection angle for each measurement has the uncertainty of 0.5° at most. Within this uncertainty, the equilibrium angle for each measurement agrees with the tilt angle 2.8° .

A. Fresh surface

First we discuss results obtained with the fresh surface. Figure 3 shows the results for three different beam energies: 3.5, 4.9, and 7 keV with the beam intensity of 50 pA. The PET capillary was tilted by $\chi=2.8^\circ$ and $\psi=0^\circ$ with respect to the incident beam direction. The observed intensities and deflection angles of the transmitted ions are plotted as functions of Q_d . The deflection angle is deduced from the mean peak position on the 2D PSD, which has the error ($\pm 0.2^\circ$). The deflection angle perpendicular to the tilt angle was constant ($\psi=0^\circ$) during the intensity evolution. So, only the deflection in the tilt direction is plotted.

The deflection angle moved toward the tilted direction in accordance with the intensity evolution. The ion guiding processes can be explained as the deflection of ions by charge patches produced on the capillary inner wall by preceding ion-surface collisions. Thus, the increase of the deflection angle during the intensity evolution should be accompanied by the growth of charge patch in the capillaries. Moreover, the decrease in the deflection angle after the maximum in Figs. 3(a) and 3(b) may be attributed to the growth of an additional secondary charge patch in the capillaries. The os-

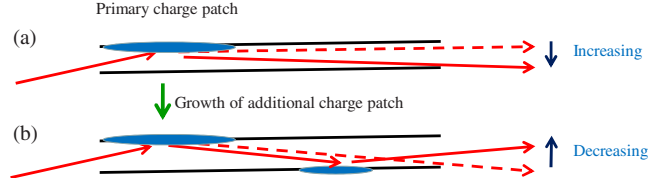


FIG. 4. (Color online) Scenario of the oscillatory behavior of the deflection angle due to the growth of charge patches.

cillatory behavior of the transmitted ions may qualitatively be explained as follows: (i) ions are deposited on the inner wall of the capillary entrance region so that it is charged up positively, (ii) the following ions are deflected by the entrance charge patch toward the capillary axis as indicated by the broken line in Fig. 4(a), (iii) with the growth of the charge patch the number of the deflected ions increases and also the deflection angle of them increases as indicated by the solid line in Fig. 4(a), (iv) with the increase of the deflection angles the ions collide with the inner wall of the capillary and create an additional charge patch as shown in Fig. 4(b), and (v) with the growth of the primary and secondary charge patches, the ions are shifted back to smaller deflection angles as indicated by the movement from the broken line to the solid line in Fig. 4(b).

For the lower incident energies of 3.5 and 4.9 keV the deflection angles of ions affected by the primary charge patch are large enough to produce the additional charge patch in the capillary as shown in Fig. 4. Previous studies [15] suggest that the equilibrium accumulated charge Q_∞ at the charge patch does not depend on the beam energy and the effective potential U produced by Q_∞ has a weak energy dependence of $(E_p/q)^{-0.3}$, where E_p is the energy and q the charge state of the ions. With increasing beam energy, the effective potential U becomes weaker [15] and the deflection angle of ions by the primary charge patch becomes smaller. Hence, the additional charge patch may not be produced. Thus, for 7 keV, the oscillatory behavior is not observed.

Very recently, Skog *et al.* [19] reported on the oscillatory behavior of the transmitted 7 keV Ne^{7+} ions through nanocapillaries in SiO_2 . They have explained the phenomenon with model calculations where charge patches are sequentially formed in the nanocapillaries. They needed three charge patches to explain the deflection angle of the transmitted ions in consistency with the aspect ratio (250:1) of the capillaries. However, in our case, the existence of two charge patches may explain the deflection angle of the transmitted ions considering the aspect ratio (60:1) of our capillaries.

The equilibrium deflection angle for 4.9 keV shown in Fig. 3(b) seems to be different from the tilt angle 2.8° . This difference may be caused by the uncertainty in the determination of the 0° value of the deflection angle. We searched the intensity maximum of the transmitted ions by changing the angles of the target holder with a weak (1 pA) beam to eliminate the beam guiding effect. Then we have set the angle of the intensity maximum as the 0° of the deflection angle. However, near the 0° very small charge patch may affect the deflection angle of the transmitted ions. Thus the determined 0° and the true one may differ by at most 0.5° , i.e., the value of the beam divergence. The equilibrium de-

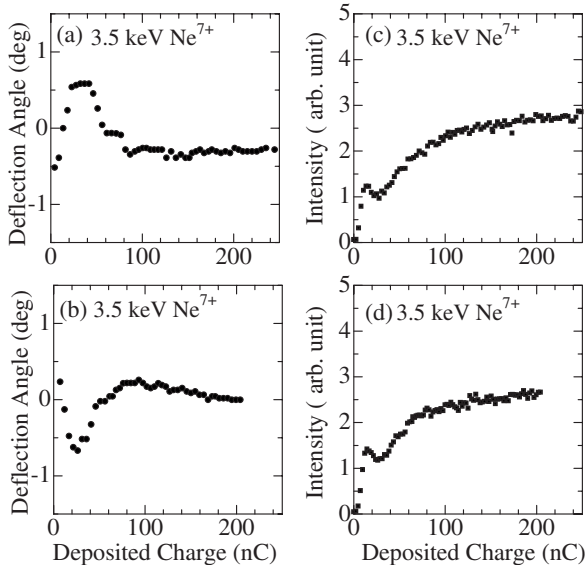


FIG. 5. Memory effect. Deflection angle (χ direction) and intensity evolution of transmitted, 3.5 keV Ne^{7+} ions as functions of charge Q_d deposited on PET surface with the tilt angle $\chi=0^\circ$. The $\psi=0^\circ$ angle is kept constant. The ion current is 50 pA. (a), (c) Precharged tilt angle $\chi=-2.8^\circ$. (b), (d) Precharged tilt angle $\chi=2.8^\circ$.

deflection angle for 4.9 keV agrees with the tilt angle within this uncertainty.

B. Charged surface

In the previous subsection, we showed evidence for the change of the charge patch from the variation of the deflection angle. Here, we present the effect of charge patches produced by precharging on the evolution of the deflection angle. Although an old charge patch is known to affect the growth of new charge patches, information reported about the memory effect is limited so far.

In Fig. 5, the intensity evolution and the deflection angle of the transmitted ions are plotted as functions of Q_d for the same tilt angle with different memory: the capillary inner walls were precharged at different tilt angles, i.e., $\chi=-2.8^\circ$ and $\chi=2.8^\circ$. In all cases $\psi=0^\circ$. Here, to simplify the experiments, the final tilt angle $\chi=0^\circ$ was chosen. The results are shown in Figs. 5(a), 5(c) and 5(b), 5(d) for the precharged tilt angles $\chi=-2.8^\circ$ and $\chi=2.8^\circ$, respectively.

After the precharging at $\chi=-2.8^\circ$, a few hours' irradiation confirming the saturation of the transmitted ion intensity, we changed the tilt angle to $\chi=0^\circ$ and measured the transmitted ions. A weak peak appeared at the deflection angle of -0.5° , which moved to 0.5° and finally approached the angle of 0° , as shown in Fig. 5(a).

The same procedure was followed again but with the saturation achieved at $\chi=2.8^\circ$. Then, we changed the tilt angle to $\chi=0^\circ$ and measured the transmitted ions. Now a weak peak appeared at the deflection angle of 0.5° and moved to -0.5° and finally approached the angle of 0° as shown in Fig. 5(b). Here, a clear oscillatory behavior is observed. For the higher beam energy of 7 keV, the oscillatory behavior became not

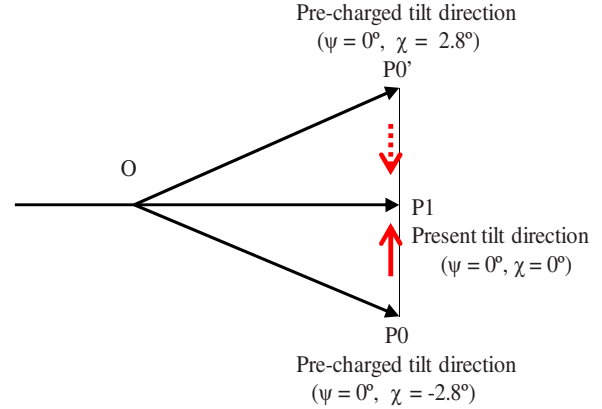


FIG. 6. (Color online) Relationship between the direction to which the peak moves and “memory” of the surface. The PET foil is located at O . $OP1$ is the present tilt direction. $OP0$ and $OP0'$ are the different precharged directions. When the ions enter the capillaries with “memory”, the deflection angle of the transmitted ions moves as indicated by the red solid arrow or the red broken arrow depending on the precharged direction. The movement may show oscillatory behavior. Finally, the ions approach the equilibrium direction around $OP1$.

so clear as in the case of the fresh surface, which can be attributed to a smaller deflection by the charge patch in the entrance region.

When ions enter the capillaries with a precharged inner wall, the ions are deflected by the charge patch in the opposite direction and collide with the inner wall. With the growth of the new charge patch and the decrease of the size of the old charge patch due to the discharge processes, the ions may be finally guided along the capillary axis passing through the capillaries. We expect that the old charge patch may also be reduced by secondary electrons produced by the creation of the new one. Hence, in this case, the old charge patch becomes smaller as the new charge patch grows. In the equilibrium conditions only the new charge patch persists guiding the ions in a self-organized manner along the capillary axis.

In Figs. 5(c) and 5(d) the intensity evolution shows a dip around $Q_d=20-40$ nC after a steep rise. In this case, the ions may be strongly deflected by the temporary charge patch so that they collide with the opposite wall where they are partially lost. For the higher energy of 7 keV, the dip is found to be less significant.

The direction to which the deflection angle of transmitted ions moves just after the start of the ion transmission, is mainly determined by the old charge patch produced by the precharging. The relationship between the ion deflection angle and the tilt angle is shown in Fig. 6. For our experimental conditions, $P0$: $\psi=0^\circ$ and $\chi=-2.8^\circ$, $P0'$: $\psi=0^\circ$ and $\chi=2.8^\circ$, and $P1$: $\psi=0^\circ$ and $\chi=0^\circ$. At the beginning of the ion guiding, a weak peak appears in between the $OP0$ ($OP0'$) and $OP1$ directions, moves to the $OP1$ direction in the $P1-O-P0$ ($P0'$) plane, as shown by the red solid (broken) arrow, and approaches the $OP1$ direction after damped oscillations.

C. Summary

In summary, we observed an oscillatory behavior in the deflection angles of ions guided by capillaries during their intensity evolutions. Oscillatory behavior in the ion deflection angle may be understood in terms of a secondary charge patch formed in addition to the main charge patch in the capillary entrance region.

ACKNOWLEDGMENTS

This work was supported by a Grant of “Developments and Applications of Exotic Quantum Beams” from RIKEN and a Grant-in-Aid for Scientific Research from Japan Society for the Promotion of Science.

-
- [1] A. Arnau, F. Aumayr, P. M. Echenique, M. Grether, W. Heiland, J. Limburg, R. Morgenstern, P. Roncin, S. Schippers, R. Schuch, N. Stolterfoht, P. Varga, T. J. M. Zouros, and H. P. Winter, *Surf. Sci. Rep.* **27**, 113 (1997).
- [2] T. Schenkel, A. V. Hamza, A. V. Barnes, and D. H. Schneider, *Prog. Surf. Sci.* **61**, 23 (1999).
- [3] *The Physics of Multiply and Highly Charged Ions*, edited by F. J. Currell (Kluwer Academic Publishers, Dordrecht, The Netherlands, 2003).
- [4] J. Burgdörfer, P. Lerner, and F. W. Meyer, *Phys. Rev. A* **44**, 5674 (1991).
- [5] S. Ninomiya, Y. Yamazaki, F. Koike, H. Masuda, T. Azuma, K. Komaki, K. Kuroki, and M. Sekiguchi, *Phys. Rev. Lett.* **78**, 4557 (1997).
- [6] Y. Morishita, R. Hutton, H. A. Torii, K. Komaki, T. Brage, K. Ando, K. Ishii, Y. Kanai, H. Masuda, M. Sekiguchi, F. B. Rosmej, and Y. Yamazaki, *Phys. Rev. A* **70**, 012902 (2004).
- [7] N. Stolterfoht, J. -H. Bremer, V. Hoffmann, R. Hellhammer, D. Fink, A. Petrov, and B. Sulik, *Phys. Rev. Lett.* **88**, 133201 (2002).
- [8] K. Schiessl, W. Palfinger, C. Lemell, and J. Burgdörfer, *Nucl. Instrum. Methods Phys. Res. B* **232**, 228 (2005).
- [9] R. Hellhammer, Z. D. Pešić, P. Sobocinski, D. Fink, J. Bundesmann, and N. Stolterfoht, *Nucl. Instrum. Methods Phys. Res. B* **233**, 213 (2005).
- [10] Gy. Viktor, R. T. Rajendra Kumar, Z. D. Pešić, N. Stolterfoht, and R. Schuch, *Nucl. Instrum. Methods Phys. Res. B* **233**, 218 (2005).
- [11] M. B. Sahana, P. Skog, G. Viktor, R. T. Rajendra Kumar, and R. Schuch, *Phys. Rev. A* **73**, 040901(R) (2006).
- [12] T. Ikeda, Y. Kanai, T. M. Kojima, Y. Iwai, T. Kambara, Y. Yamazaki, M. Hoshino, T. Nebiki, and T. Narusawa, *Appl. Phys. Lett.* **89**, 163502 (2006).
- [13] T. Ikeda, Y. Kanai, T. M. Kojima, Y. Iwai, Y. Kanazawa, M. Hoshino, T. Kobayashi, G. P. Pokhil, and Y. Yamazaki, *J. Phys.: Conf. Ser.* **88**, 012031 (2007).
- [14] N. Stolterfoht, R. Hellhammer, Z. D. Pešić, V. Hoffmann, J. Bundesmann, A. Petrov, D. Fink, B. Sulik, M. Shah, K. Dunn, J. Pedregosa, and R. W. McCullough, *Nucl. Instrum. Methods Phys. Res. B* **225**, 169 (2004).
- [15] N. Stolterfoht, R. Hellhammer, J. Bundesmann, and D. Fink, *Phys. Rev. A* **77**, 032905 (2008).
- [16] Y. Kanai, M. Hoshino, T. Kambara, T. Ikeda, R. Hellhammer, N. Stolterfoht, and Y. Yamazaki, *Nucl. Instrum. Methods Phys. Res. B* **258**, 155 (2007).
- [17] N. Stolterfoht, R. Hellhammer, J. Bundesmann, D. Fink, Y. Kanai, M. Hoshino, T. Kambara, T. Ikeda, and Y. Yamazaki, *Phys. Rev. A* **76**, 022712 (2007).
- [18] M. Fürsatz, W. Meissl, S. Pleschko, I. C. Gebeshuber, N. Stolterfoht, H. P. Winter, and F. Aumayr, *J. Phys.: Conf. Ser.* **58**, 319 (2007).
- [19] P. Skog, H. Q. Zhang, and R. Schuch, *Phys. Rev. Lett.* **101**, 223202 (2008).
- [20] K. Schiessl, W. Palfinger, K. Tökési, H. Nowotny, C. Lemell, and J. Burgdörfer, *Phys. Rev. A* **72**, 062902 (2005).
- [21] Y. Kanai, D. Dumitriu, Y. Iwai, T. Kambara, T. M. Kojima, A. Mohri, Y. Morishita, Y. Nakai, H. Oyama, N. Oshima, and Y. Yamazaki, *Phys. Scr.* **T92**, 467 (2001).
- [22] Y. Yamazaki, S. Ninomiya, F. Koike, H. Masuda, T. Azuma, K. Komaki, K. Kuroki, and M. Sekiguchi, *J. Phys. Soc. Jpn.* **65**, 1199 (1996).
- [23] K. Tökési, L. Wirtz, C. Lemell, and J. Burgdörfer, *Phys. Rev. A* **61**, 020901(R) (2000).